current issues in molecular biology

MDPI

Article

Effects of *Papenfussiella kuromo* Extract on Inflammatory Markers and NF-κB-Associated Proteins in *Porphyromonas gingivalis*-Stimulated RAW 264.7 Macrophages

Min-jeong Kim [1], Tuan Quoc Nguyen [2] and Hyun-jin Kim [3,*]

[1] Department of Convergence Technology for Food Industry, Wonkwang University, Iksan 54538, Republic of Korea; lucklove519@naver.com
[2] Department of Oriental Pharmacy, Wonkwang-Oriental Medicines Research Institute, College of Pharmacy, Wonkwang University, Iksan 54538, Republic of Korea; quoctuan301281@gmail.com
[3] Department of Oral Anatomy, Institute of Biomaterial Implant, School of Dentistry, Wonkwang University, Iksan 54538, Republic of Korea
* Correspondence: khjin1005@wku.ac.kr

Abstract

Periodontitis is a chronic inflammatory disease characterized by progressive destruction of periodontal supporting tissues resulting from dysregulated host immune responses to periodontal pathogens. Modulation of host inflammatory signaling pathways has thus emerged as a promising therapeutic strategy for periodontal disease. In this study, we investigated the anti-inflammatory effects of *Papenfussiella kuromo* (*P. kuromo*) extract on *Porphyromonas gingivalis* (*P. gingivalis*)-induced inflammation in RAW 264.7 macrophages. Cell viability was assessed after treatment with the extract alone using an MTS assay; nitric oxide (NO) production was measured by the Griess reaction; inducible nitric oxide synthase (iNOS) expression and NF-κB signaling activation were analyzed by Western blotting; and mRNA levels of pro-inflammatory cytokines (IL-1β, IL-6, and TNF-α) were quantified by qRT-PCR. *P. kuromo* extract showed no cytotoxicity toward RAW 264.7 macrophages within the selected concentration range. In *P. gingivalis*-stimulated cells, the extract significantly reduced NO production and suppressed iNOS protein expression. Moreover, *P. kuromo* extract downregulated IL-1β, IL-6, and TNF-α mRNA in a concentration-dependent manner. At 24 h, lower IKKα/β and IκBα phosphorylation and reduced nuclear accumulation of NF-κB p65 were also observed. Whether these NF-κB-associated changes contributed to the reductions in inflammatory markers remains to be determined. The relevance of these findings to periodontal disease should be evaluated in future studies using more physiologically relevant models.

Keywords: periodontitis; *Papenfussiella kuromo*; *Porphyromonas gingivalis*; RAW 264.7 macrophages; anti-inflammatory effects

Check for updates

Academic Editor: Chan-Yen Kuo

Received: 20 October 2026
Revised: 20 November 2026
Accepted: 21 November 2026
Published: 25 November 2026

Copyright: © 2026 by the authors. Licensee MDPI, Basel, Switzerland. This article is an open access article distributed under the terms and conditions of the Creative Commons Attribution (CC BY) license.

1. Introduction

Periodontitis is a prevalent chronic inflammatory disease characterized by progressive destruction of the tooth-supporting apparatus, leading to alveolar bone loss and eventual tooth loss [1]. Contemporary models of periodontitis emphasize that dysbiotic microbial communities provide the initiating trigger; however, the clinical trajectory of disease-tissue breakdown versus stability-depends predominantly on the magnitude and persistence of the host immune and inflammatory responses [2]. In this context, periodontitis can be regarded as a disorder of immune homeostasis, wherein inflammatory responses originally

intended for host protection become maladaptive, self-sustaining, and osteodestructive [3]. A central hallmark of periodontitis is the persistent production of pro-inflammatory mediators (e.g., tumor necrosis factor-α (TNF-α), interleukin-1β (IL-1β), IL-6) and downstream effectors such as nitric oxide (NO) and prostaglandin E2 (PGE2), which collectively amplify leukocyte recruitment, vascular activation, and matrix degradation [4]. Importantly, inflammation in periodontitis is not merely "excessive" but frequently fails to resolve [5]. Resolution is an active, orchestrated process governed by pro-resolving mediators and cellular reprogramming; when this resolution is impaired, inflammatory circuits remain locked in an activated state, driving chronic tissue injury [6]. This resolution-failure perspective is particularly relevant to periodontal tissues, where repeated microbial challenges and mechanical stress converge with host factors (e.g., metabolic dysregulation, aging-associated "inflammaging") to perpetuate an inflammatory microenvironment [7].

From an osteoimmunology perspective, periodontal destruction is propelled by immune–bone crosstalk [8]. Pro-inflammatory cytokines and pattern-recognition receptor signaling promote osteoclastogenesis directly and indirectly, notably through modulation of the RANKL/OPG axis and inflammatory amplification loops [9]. Macrophages, as key sensors and amplifiers of microbial and danger signals, integrate these cues and shape the local cytokine landscape [10]. A shift toward a pro-inflammatory macrophage phenotype, together with sustained activation of intracellular signaling hubs such as nuclear factor-kappa B (NF-κB) and mitogen-activated protein kinases (MAPKs: ERK, JNK, p38), maintains transcriptional programs that favor tissue breakdown [11]. In parallel, inflammasome-associated pathways (e.g., NLRP3–caspase-1) can potentiate IL-1β maturation, further entrenching inflammatory destruction [12]. Collectively, these converging pathways highlight why periodontitis is increasingly framed as a disease that benefits from host response rebalancing, rather than pathogen elimination alone [13].

Standard periodontal therapy is primarily based on mechanical debridement to reduce microbial burden, with adjunctive antimicrobials or anti-inflammatory drugs used selectively [14]. While such approaches can be effective, they have inherent limitations. Antibiotics raise concerns regarding resistance and ecological perturbation of the oral microbiome, whereas broad-spectrum anti-inflammatory drugs may suppress protective immune functions or interfere with tissue repair [15]. These clinical limitations have driven interest in host-modulating therapy (HMT) as a complementary strategy [16]. Unlike indiscriminate immunosuppression, HMT aims to attenuate destructive inflammatory signaling while preserving essential host defenses and enabling restoration of tissue homeostasis [17]. In periodontitis, an ideal HMT agent would (i) dampen overactive NF-κB/MAPK signaling, (ii) reduce pathological mediator production (e.g., IL-1β, IL-6, TNF-α, iNOS/COX-2 products), (iii) favor resolution-associated cellular states (e.g., macrophage functional reprogramming), and (iv) ultimately mitigate osteodestructive coupling [18].

Marine macroalgae represent a rich reservoir of structurally diverse bioactives, including polyphenols, sulfated polysaccharides, glycolipids, and other metabolites, many of which have shown immunomodulatory potential [19]. Among these, *P. kuromo* is a marine alga documented in intertidal seaweed surveys in Korea and has attracted scientific interest in non-oral inflammatory contexts [20]. Notably, an earlier in vitro study reported anti-inflammatory activity of *P. kuromo* extract in LPS- and peptidoglycan-stimulated RAW 264.7 macrophage activation models, supporting the plausibility that *P. kuromo* contains constituents capable of regulating inflammatory mediator production [21]. Unlike that study, the present work examines *P. kuromo* extract in RAW 264.7 macrophages exposed to a heat-treated whole-bacterial preparation of the periodontal pathogen *P. gingivalis*.

Periodontal inflammation is triggered not only by generic endotoxin exposure but also by specific periodontal pathogen-associated patterns, including *P. gingivalis*-derived

LPS and associated virulence factors that may engage Toll-like receptors and other innate sensors in a context-dependent manner [22,23]. For example, epiloliolide isolated from *Sargassum horneri* has been evaluated in human periodontal ligament cells stimulated with *P. gingivalis* LPS [24].

In this study, we investigated the effects of *P. kuromo* extract on inflammatory responses in *P. gingivalis*-stimulated RAW 264.7 macrophages. Using an in vitro model in which macrophages were exposed to a heat-treated whole-bacterial preparation of P. gingivalis, we examined (i) cell viability following extract treatment, (ii) nitrite accumulation, pro-inflammatory cytokine mRNA expression, and iNOS protein expression, and (iii) changes in NF-κB-associated proteins, including IKK and IκBα phosphorylation and the subcellular distribution of p65. Together, these analyses provide preliminary in vitro evidence to warrant further investigation of *P. kuromo* extract in periodontal inflammation models.

2. Materials and Methods

2.1. Chemicals and Reagents

Dulbecco's Modified Eagle's medium (DMEM), fetal bovine serum (FBS), and antibiotic–antimycotic solution were obtained from Gibco BRL (Life Technologies, Carlsbad, CA, USA). The CellTiter 96 AQueous One Solution Cell Proliferation Assay kit and Griess Reagent System were purchased from Promega (Madison, WI, USA). Oligonucleotide primers for IL-1β, IL-6, TNF-α, and β-actin were synthesized by Bioneer (Daejeon, Republic of Korea). Antibodies against iNOS, phosphorylated IκB kinase (IKK)α/β (p-IKKα/β), IKKα, IKKβ, phosphorylated NF-κB inhibitor α (IκBα) (p-IκBα), IκBα, and the NF-κB p65 subunit were obtained from Cell Signaling Technologies (Danvers, MA, USA). Antibodies targeting β-actin and proliferating cell nuclear antigen (PCNA) were purchased from Sigma-Aldrich (St. Louis, MO, USA) and Santa Cruz Biotechnology (Dallas, TX, USA), respectively. Horseradish peroxidase (HRP)-conjugated secondary anti-rabbit IgG was obtained from Cell Signaling Technologies (Danvers, MA, USA).

2.2. Preparation of Heat-Treated P. gingivalis

P. gingivalis was provided by OraTix Inc. (Seoul, Republic of Korea) as a heat-treated whole-bacterial preparation. According to the preparation information provided by OraTix, the bacterial suspension was harvested by centrifugation and washed twice with phosphate-buffered saline (PBS). Bacterial density was estimated from OD_{600} measurements, and the suspension was diluted accordingly; an OD_{600} of 0.5 was taken to correspond to approximately 5×10^8 bacteria/mL. The suspension was heat-treated at 80 °C for 30 min. A single batch of the preparation was used throughout this study. For macrophage stimulation, the preparation was diluted to a final estimated concentration equivalent to 1×10^8 bacteria/mL, based on the OD_{600} measurement before heat treatment.

2.3. P. kuromo Extract

The *P. kuromo* extract analyzed in this study was provided by Professor Han-Gil Choi from the Department of Biological Sciences at Wonkwang University. *P. kuromo* samples were collected from Ihoijin, Jangheung (34°27′ N, 126°56′ E), on the southern coast of the Republic of Korea. The collected samples were washed thoroughly with tap water to remove foreign substances and dried at room temperature (20 °C). The dried sample was ground into a fine powder using a mixer. The powdered sample was then immersed in 94% ethanol [10-fold (*v*/*w*)] and extracted three times over 2 days at room temperature. The extract was filtered, concentrated using a vacuum rotary evaporator (Eyela N-1000, Tokyo, Japan), and subsequently lyophilized using a freeze-dryer (Ilshin TFD5505, Dongducheon, Republic of Korea). The final lyophilized powder of *P. kuromo* extract was dissolved in dimethyl

sulfoxide (DMSO) to prepare a stock solution and stored at −20 °C until further use. The same batch of *P. kuromo* extract was used for HPLC analysis and the cell-based experiments.

2.4. HPLC Analysis

HPLC analysis of *P. kuromo* extract was conducted using YL9100 HPLC system (Young Lin Instrument Co., Ltd., Anyang, Republic of Korea). Chromatographic separation was achieved using a Kinetex C18 column (5 µm, 150 × 4.6 mm) (Phenomenex Inc., Torrance, CA, USA) set at 25 °C. A 10 µL sample was injected and eluted at a flow rate of 0.7 mL/min. The mobile phase system consisted of 0.1% formic acid in distilled water (buffer A) and 0.1% formic acid in acetonitrile (buffer B). The elution was performed using a linear gradient from 10% to 100% B over 45 min. The eluate was monitored by UV detection at 254 nm.

2.5. Cell Culture

RAW 264.7 murine macrophage cells were obtained from the American Type Culture Collection (TIB-71, ATCC, Rockville, MD, USA) and maintained in DMEM supplemented with 10% fetal bovine serum (Gibco BRL) and 1% antibiotic–antimycotic solution (Gibco BRL). The cells were incubated at 37 °C in a humidified atmosphere containing 5% CO_2. The cells were subcultured and plated at 80% confluency. For the inflammatory stimulation experiments, cells were incubated in serum-free DMEM during the 24 h exposure to the heat-treated *P. gingivalis* preparation.

2.6. Cell Viability Assay

Cell viability was evaluated using the 3-(4,5-dimethylthiazol-2-yl)-5-(3-carboxymethoxyphenyl)-2-(4-sulfophenyl)-2H-tetrazolium (MTS) assay (CellTiter 96® AQueous One Solution Cell Proliferation Assay, Promega, Madison, WI, USA). Briefly, RAW 264.7 macrophages were seeded in 96-well plates at a density of 1×10^5 cells/well and incubated overnight for cell attachment. The cells were then treated with various concentrations (15–250 µg/mL) of *P. kuromo* extract or vehicle only and incubated at 37 °C in a 5% CO_2 atmosphere for 24 h. Afterward, MTS solution was added to each well at a 1:5 ratio, and the plates were incubated for an additional 2 h at 37 °C in a humidified 5% CO_2 incubator. Absorbance was measured at 490 nm using a microplate reader (TECAN, Männedorf, Zurich, Switzerland).

2.7. NO Assay

RAW 264.7 macrophages were plated at a density of 5×10^5 cells/well in 24-well plates and incubated overnight at 37 °C in a humidified 5% CO_2 incubator (Thermo Fisher Scientific, Rockford, IL, USA). The cells were pre-treated with various concentrations (15–125 µg/mL) of *P. kuromo* extract for 2 h, followed by stimulation with 1×10^8 bacteria/mL of *P. gingivalis* for 24 h. After incubation, the cell culture supernatant (50 µL) was mixed with an equal volume of Griess reagent (Promega, Madison, WI, USA) and incubated at room temperature for 10 min. NO production was quantified by measuring the absorbance at 540 nm using a microplate reader. A sodium nitrite ($NaNO_2$) standard curve was used to calculate NO concentrations.

2.8. RNA Isolation and Quantitative Real-Time PCR (qRT-PCR)

To assess transcriptional changes, RAW 264.7 macrophages were inoculated into 24-well culture plates at a density of 5×10^5 cells/well and allowed to adhere overnight under standard conditions (37 °C, 5% CO_2 in a humidified incubator). Cells were subjected to a 2 h pre-treatment with various concentrations of *P. kuromo* extract (15, 30, and 60 µg/mL), followed by exposure to *P. gingivalis* (1×10^8 bacteria/mL) for a 24 h incubation period. Total cellular RNA was isolated using TRIzol reagent (Ambion, Carlsbad, CA, USA) ac-

cording to the manufacturer's instructions. The quantity and quality of the extracted RNA were verified using a Biospec-Nano spectrophotometer (Shimadzu, Nakagyo-ku, Kyoto, Japan). Subsequently, cDNA was synthesized from the purified RNA templates via the PrimeScript RT Reagent Kit (TaKaRa, Shiga, Japan) according to the manufacturer's protocol. Quantitative real-time PCR amplification was performed using Power SYBR Green PCR Master Mix (Applied Biosystems, Warrington, UK) on a StepOnePlus Real-Time PCR platform (Applied Biosystems, Foster City, CA, USA). The thermal profile consisted of an initial denaturation phase at 95 °C for 10 min, followed by 40 cycles of denaturation at 95 °C for 15 s and annealing/extension at 60 °C for 1 min. Cycle threshold (Ct) values were derived from the exponential amplification curves. The relative transcription levels of target genes (IL-1β, IL-6, and TNF-α) were normalized against β-actin mRNA expression, which served as the internal reference control. The primer sequences used were as follows: IL-1β (NM_008361): Forward: 5′-GAAAGACGGCACACCCACCCT-3′ and Reverse: 5′-GCTCTGCTTGTGAGGTGCTGATGTA-3′; IL-6 (NM_031168): Forward: 5′-GATGGATGCTACCAAACTGGA-3′ and Reverse: 5′-TCTGAAGGACTCTGGCTTTG-3′; TNF-α (BC137720): Forward: 5′-CCACCACGCTCTTCTGTCTAC-3′ and Reverse: 5′-AGGGTCTGGGCCATAGAACT-3′; β-actin (NM_007393): Forward: 5′-CATCACTATTGGCA ACGAGC-3′ and Reverse: 5′-GACAGCACTGTGTTGGCATA-3′.

2.9. Western Blot Analysis

For protein expression analysis, RAW 264.7 macrophages were seeded in 6-well plates and treated with indicated concentrations of *P. kuromo* extract (15, 30, and 60 μg/mL) and *P. gingivalis* (1×10^8 bacteria/mL) for 24 h. Following incubation, cells were collected and rinsed twice with ice-cold phosphate-buffered saline (Gibco, Grand Island, NY, USA). Cytoplasmic and nuclear protein fractions were isolated using a Nuclear Extraction Kit (Cayman, Ann Arbor, MI, USA) to evaluate nuclear translocation. Protein concentrations within the respective lysates were determined using the Pierce™ BCA Protein Assay Kit (Thermo Fisher Scientific, Rockford, IL, USA). Equal amounts of quantified proteins were resolved via 10% sodium dodecyl sulfate-polyacrylamide gel electrophoresis (SDS-PAGE) and electro-transferred onto polyvinylidene fluoride membranes (Amersham Biosciences, Piscataway, NJ, USA). Non-specific binding sites were blocked by incubating the membranes with 5% skim milk for 1 h at room temperature, followed by three washes with Tris-buffered saline containing 0.1% Tween 20 (TBS-T). The membranes were then probed overnight at 4 °C with specific primary antibodies diluted as follows: iNOS (1:1000), NF-κB p65 subunit (1:1000), p-IκBα (1:1000), IκBα (1:1000), p-IKKα/β (1:1000), and β-actin (1:5000). After thorough washing with TBS-T, the membranes were exposed to horseradish peroxidase (HRP)-conjugated secondary antibodies for 1 h at room temperature. Immunoreactive bands were detected using Immobilon Western Chemiluminescent HRP Substrate (Millipore, Billerica, MA, USA), captured via cSeries Capture Software version 2.1.4.0731 (Azure Biosystems, Dublin, CA, USA), and densitometrically quantified using ImageJ 1.52a software (NIH, Bethesda, MD, USA).

2.10. Statistical Analysis

Statistical analyses were performed using SPSS software version 25.0 (SPSS Inc., Chicago, IL, USA). All quantitative data are expressed as the mean ± standard deviation (SD) from a minimum of three independent replicate experiments. To determine the significance of differences between experimental groups, differences between groups were analyzed using Student's *t*-test. A p-value < 0.05 was considered statistically significant.

3. Results

3.1. HPLC Analysis of P. kuromo Extract

To characterize the chemical complexity of the *P. kuromo* extract and provide a rationale for evaluating the crude extract rather than individual isolated compounds, a full-scan HPLC analysis was conducted. The resulting chromatographic profile exhibited 51 distinct peaks, indicating the presence of a diverse range of constituents with varying retention times. Among these, the most prominent peak was detected at 1.925 min, with a peak area of 565.734 (mv.s) corresponding to 19.9% of the total chromatographic area. Other major peaks were observed at retention times of 2.583 min and 17.767 min, accounting for 9.4% and 13.9%, respectively. Overall, the detected compounds exhibited retention times ranging from 1.925 to 44.808 min (Figure 1). The number of chromatographic signals and broad distribution of retention times demonstrate the chemical complexity of the *P. kuromo* extract and suggest the coexistence of multiple bioactive constituents, which may contribute to potential synergistic effects within the crude extract.

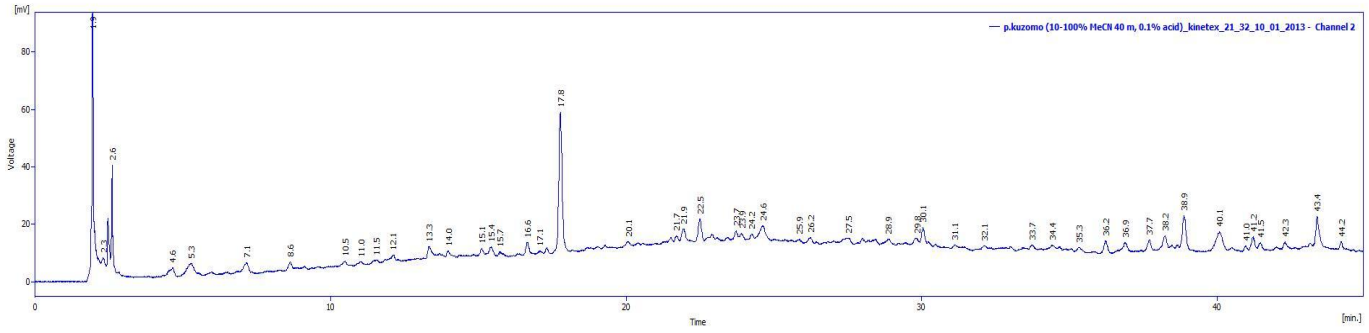


Figure 1. HPLC chromatogram of the crude extract of *P. kuromo*. HPLC analysis of *P. kuromo* extract was conducted using a Kinetex C18 column (5 µm, 150 × 4.6 mm) maintained at 25 °C. The analysis was performed at a flow rate of 0.7 mL/min with the detection wavelength set at 254 nm.

3.2. Effect of P. kuromo Extract on the Viability of RAW 264.7 Macrophages

To determine whether *P. kuromo* extract exerts cytotoxic effects on RAW 264.7 macrophages, an MTS assay was performed. The cells were treated with various concentrations of the extract, ranging from 15 to 250 µg/mL, for 24 h. As illustrated in Figure 2, *P. kuromo* extract did not exert any significant cytotoxic effects at concentrations up to 125 µg/mL, with cell viability consistently remaining above 100% relative to the untreated control group. At the maximum tested concentration of 250 µg/mL, a slight decrease in cell proliferation was noted, with viability maintained at approximately 77.2%. These viability results reflect extract-only treatment and do not establish cell viability under the combined *P. gingivalis* stimulation and extract-treatment conditions used in the subsequent assays.

3.3. Suppressive Effect of P. kuromo Extract on P. gingivalis-Induced NO Production

To evaluate the anti-inflammatory potential of *P. kuromo* extract, the production of NO was quantified in RAW 264.7 macrophages stimulated with *P. gingivalis* using the Griess reaction. As illustrated in Figure 3, stimulation with *P. gingivalis* triggered a robust increase in NO release into the culture medium compared to the baseline levels observed in the untreated control group. However, pretreatment with *P. kuromo* extract significantly attenuated this *P. gingivalis*-induced NO production in a dose-dependent manner. In particular, the extract markedly reduced NO concentrations, with the largest reduction observed at 125 µg/mL. A reduction was also observed at 60 µg/mL. The subsequent iNOS, cytokine mRNA, and NF-κB analyses were conducted at 15, 30, and 60 µg/mL, whereas 125 µg/mL was evaluated in the

NO assay only. These data indicate that *P. kuromo* extract reduced nitrite accumulation in *P. gingivalis*-stimulated RAW 264.7 macrophages under the conditions tested.

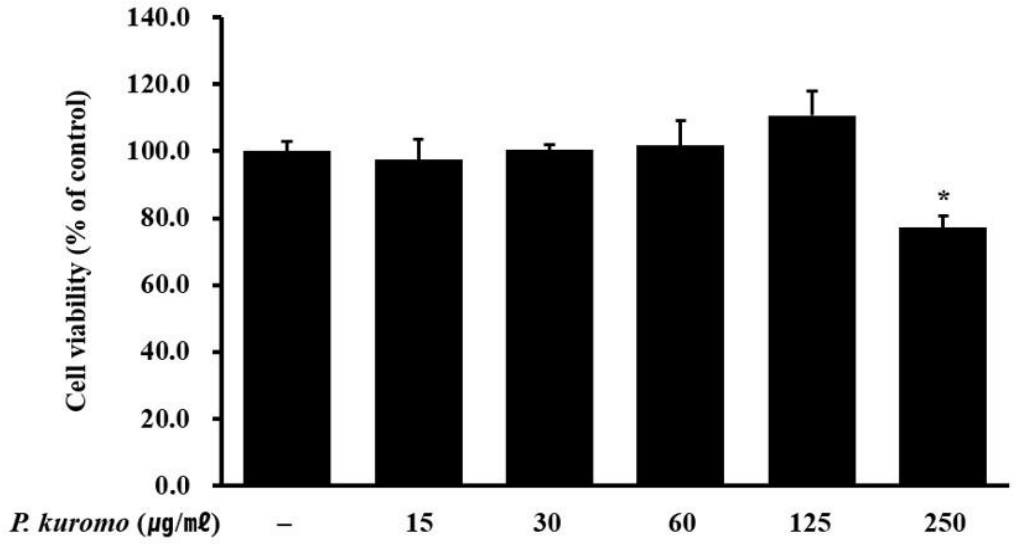


Figure 2. Cytotoxicity of *P. kuromo* extract on RAW 264.7 macrophages. Cells were treated with various concentrations (15–250 μg/mL) of the extract for 24 h, and cell viability was quantified via an MTS assay. Vehicle only served as the control (100%). Data are presented as the mean ± standard deviation (SD) of three independent experiments. * $p < 0.05$ indicates a statistically significant difference compared with the untreated control group.

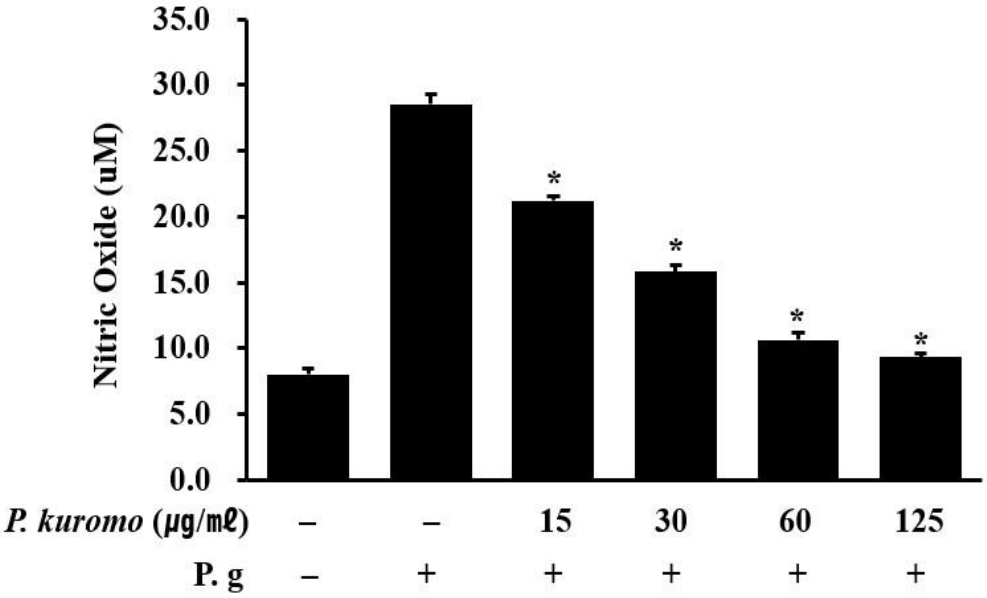


Figure 3. Inhibitory effect of *P. kuromo* extract on NO production in activated RAW 264.7 macrophages. Cells were stimulated with *P. gingivalis* (1×10^8 bacteria/mL) for 24 h in the presence or absence of *P. kuromo* extract at indicated concentrations (15–125 μg/mL). The levels of NO in the culture supernatants were determined using the Griess reagent system. Data are presented as the mean ± standard deviation (SD) of triplicate experiments. * $p < 0.05$ indicates a statistically significant difference compared with the *P. gingivalis*-stimulated group.

3.4. Inhibitory Effect of P. kuromo Extract on P. gingivalis-Induced iNOS Protein Expression

iNOS is the principal rate-limiting enzyme responsible for the high-output production of NO during pathological inflammatory responses. To determine whether the suppressive

effect of *P. kuromo* extract on NO generation was associated with modulation of iNOS protein expression, Western blot analysis was performed. As shown in Figure 4, stimulation with *P. gingivalis* (1×10^8 bacteria/mL) led to a robust and significant upregulation of iNOS protein expression in RAW 264.7 macrophages compared with the untreated control group. Conversely, pre-treatment with *P. kuromo* extract markedly diminished iNOS protein levels in a concentration-dependent manner at concentrations of 15, 30, and 60 μg/mL. β-actin was used as an internal loading control, and its stable expression confirmed the specificity of iNOS downregulation. These findings indicate that the suppression of NO production by *P. kuromo* extract is mediated through suppression of iNOS at the transcriptional and/or translational level.

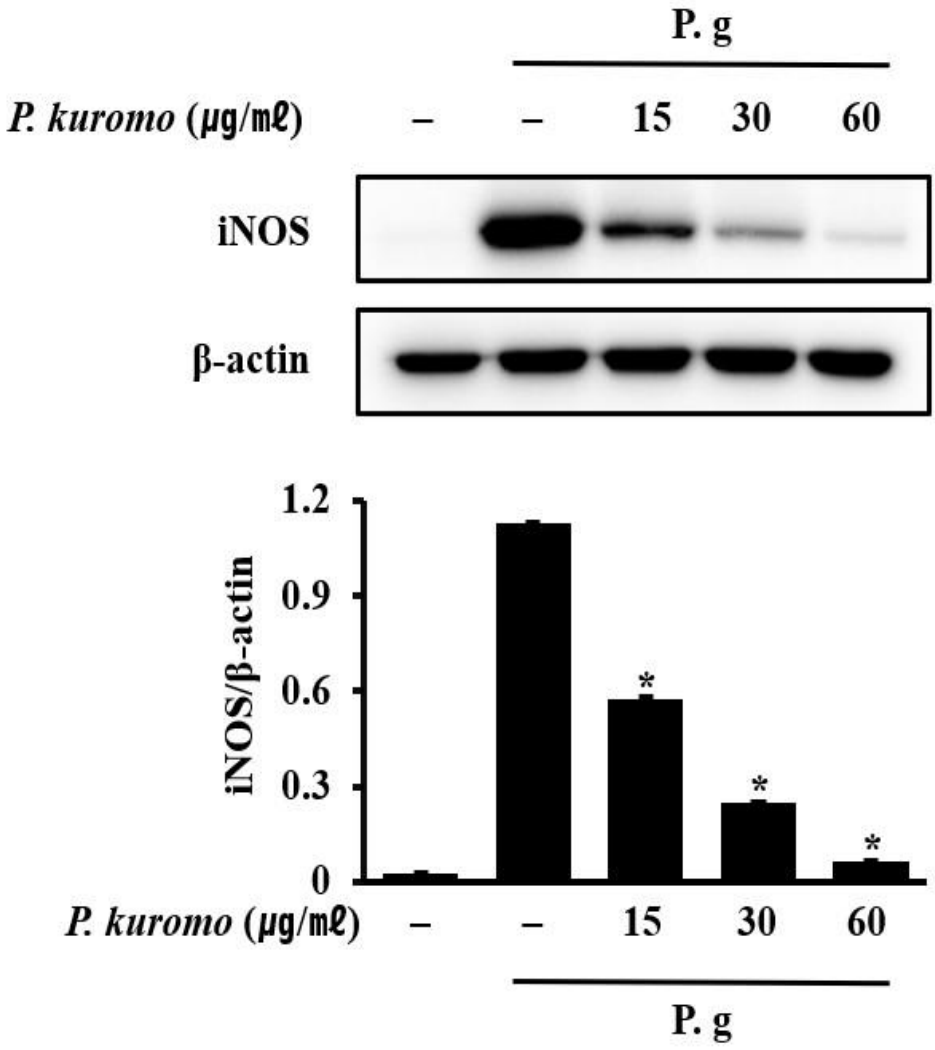


Figure 4. Attenuation of *P. gingivalis*-induced iNOS protein expression by *P. kuromo* extract. RAW 264.7 macrophages were pre-treated with indicated concentrations (15, 30, and 60 μg/mL) of *P. kuromo* extract for 2 h and then stimulated with *P. gingivalis* (1×10^8 bacteria/mL) for 24 h. Total cellular proteins were extracted, and iNOS protein levels were analyzed by Western blotting. β-actin was employed as the internal loading control to normalize protein levels. Data are expressed as the mean ± standard deviation (SD) of three independent experiments. * $p < 0.05$ indicates a statistically significant difference compared with the *P. gingivalis*-stimulated group.

3.5. Inhibitory Effect of P. kuromo Extract on P. gingivalis-Induced Pro-Inflammatory Cytokine mRNA Expression

To further examine the anti-inflammatory mechanism of *P. kuromo* extract, its effect on the transcriptional activation of key pro-inflammatory cytokines was assessed by quantitative real-time PCR (qRT-PCR). As shown in Figure 5A–C, stimulation of RAW 264.7 macrophages with *P. gingivalis* (1×10^8 bacteria/mL) markedly increased the mRNA expression of IL-1β, IL-6, and TNF-α compared with the untreated control group. Importantly, pre-treatment with *P. kuromo* extract counteracted this pathogen-induced transcriptional increase and reduced the mRNA levels of all three cytokines in a concentration-dependent manner. At the maximum non-cytotoxic concentration of 60 μg/mL, the extract showed the strongest inhibitory effect, reducing the elevated IL-1β, IL-6, and TNF-α mRNA levels toward baseline. These results indicate that *P. kuromo* extract suppresses the transcriptional activation of key pro-inflammatory cytokines in macrophages and attenuates the early amplification phase of the periodontal inflammatory response.

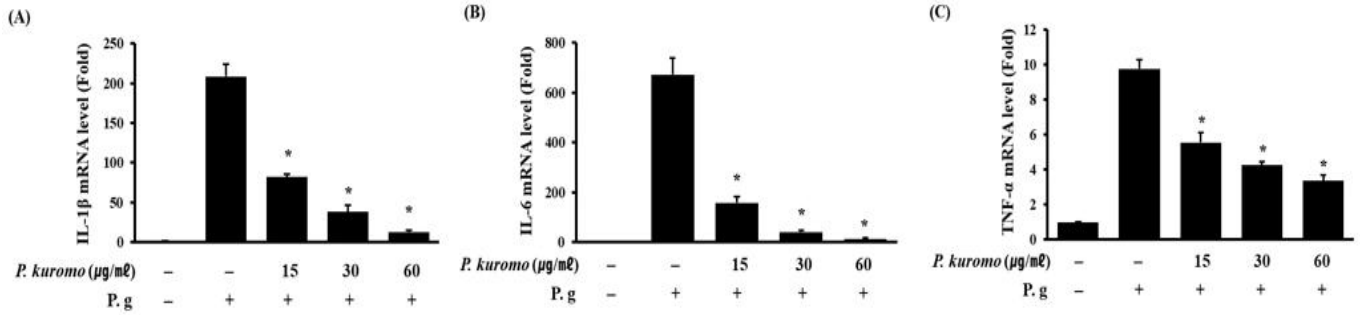


Figure 5. Down-regulation of *P. gingivalis*-induced pro-inflammatory cytokine mRNA expression by *P. kuromo* extract. RAW 264.7 macrophages were pre-treated with specified concentrations (15, 30, and 60 μg/mL) of *P. kuromo* extract for 2 h and then exposed to *P. gingivalis* (1×10^8 bacteria/mL) for 24 h. The transcriptional levels of (**A**) IL-1β, (**B**) IL-6, and (**C**) TNF-α were quantified via quantitative real-time PCR (qRT-PCR). β-actin was used as the internal reference standard to normalize the relative fold changes. Data are represented as the mean ± standard deviation (SD) of three independent experiments. * $p < 0.05$ indicates a statistically significant difference compared with the *P. gingivalis*-stimulated, extract-untreated group.

3.6. Inhibitory Effect of P. kuromo Extract on the Activation of the NF-κB Signaling Pathway

The NF-κB signaling cascade is a central transcriptional hub that regulates the expression of downstream pro-inflammatory enzymes and cytokines during periodontal pathogenesis. To elucidate the molecular mechanism underlying the anti-inflammatory activity of *P. kuromo* extract, we examined the activation of upstream signaling molecules and the nuclear translocation of the NF-κB p65 subunit by Western blot analysis. As shown in Figure 6, after 24 h of exposure to the heat-treated *P. gingivalis* preparation, RAW 264.7 macrophages exhibited higher levels of phosphorylated IKKα/β and IκBα, lower levels of total IκBα, and greater nuclear accumulation of p65 than unstimulated cells. Pretreatment with *P. kuromo* extract (15, 30, and 60 μg/mL) was associated with lower IKKα/β and IκBα phosphorylation, higher total IκBα levels, and reduced nuclear accumulation of p65 at this time point. These findings show differences in NF-κB-associated protein levels and p65 subcellular distribution at 24 h; they do not establish the sequence or timing of earlier signaling events.

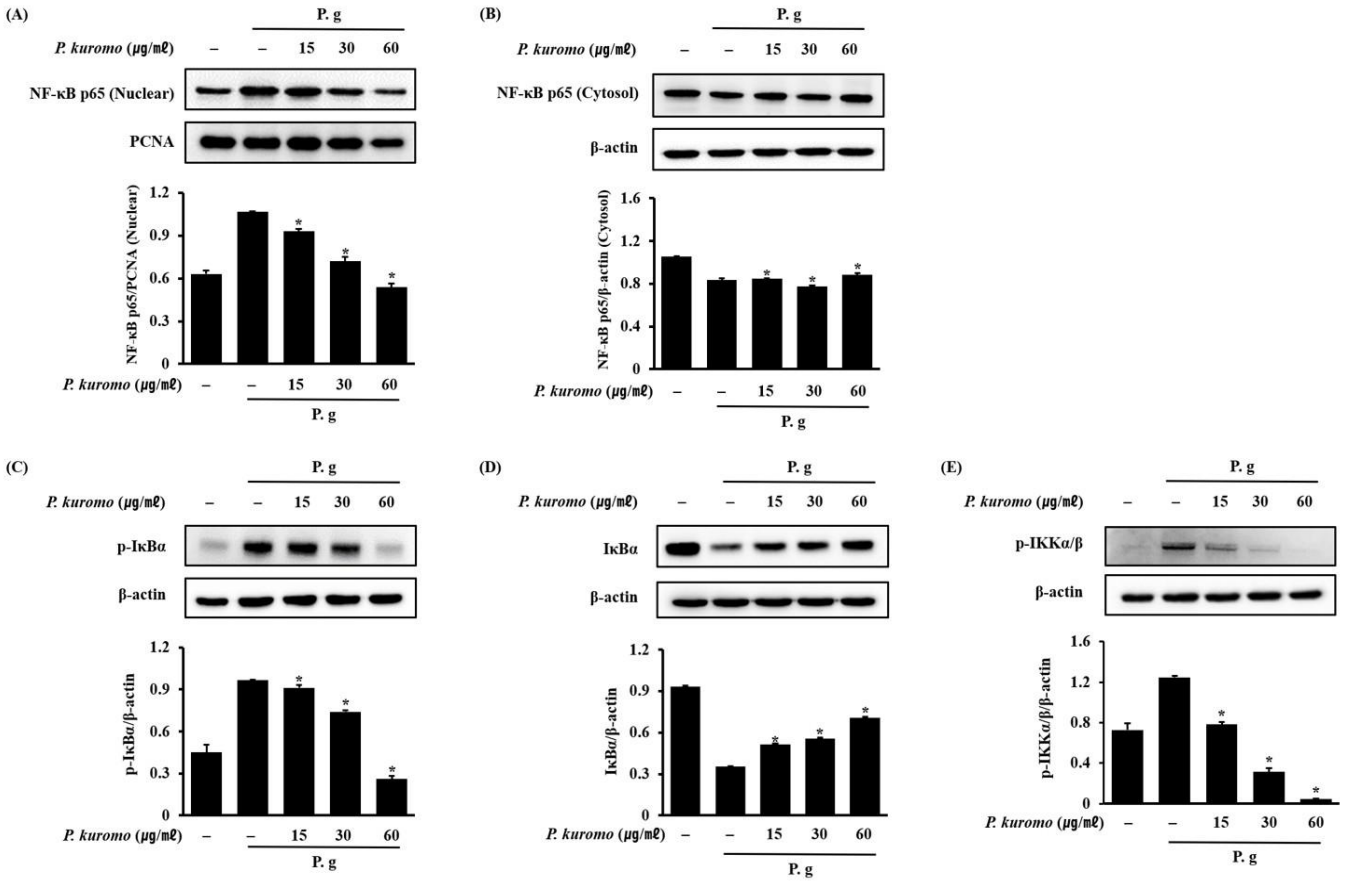


Figure 6. Suppression of *P. gingivalis*-induced NF-κB signaling activation and p65 nuclear translocation by *P. kuromo* extract. RAW 264.7 macrophages were pre-treated with specified concentrations (15, 30, and 60 μg/mL) of *P. kuromo* extract for 2 h and then stimulated with *P. gingivalis* (1×10^8 bacteria/mL) for 24 h. Protein levels of (**A**) nuclear NF-κB p65, (**B**) cytosolic NF-κB p65, (**C**) phosphorylated IκBα, (**D**) total IκBα, and (**E**) phosphorylated IKKα/β were determined via Western blotting. β-actin was used as the loading control for the cytosolic and whole-cell fractions, and proliferating cell nuclear antigen (PCNA) was used as the loading control for the nuclear fraction. Data are shown as the mean ± standard deviation (SD) of triplicate experiments. * $p < 0.05$ indicates a statistically significant difference compared with the *P. gingivalis*-stimulated, extract-untreated group.

4. Discussion

Periodontitis is a prevalent chronic inflammatory disease characterized by a dysregulated host immune response to periodontal pathogens, ultimately leading to progressive destruction of the tooth-supporting apparatus and eventual tooth loss [1,3]. Accumulating evidence over the past decade underscores that the clinical trajectory of periodontal tissue breakdown is governed predominantly by the magnitude, duration, and persistence of the host-derived immune–inflammatory cascade rather than the mere presence of periodontal pathogens alone [2,13]. Consequently, host-modulating therapy (HMT) has emerged as a promising therapeutic strategy to complement conventional mechanical debridement [14,16]. In this study, we evaluated the anti-inflammatory effects of *P. kuromo* extract in a *P. gingivalis*-stimulated in vitro model of periodontal inflammation. In this in vitro model, *P. kuromo* extract reduced nitrite accumulation, iNOS protein expression, and pro-inflammatory cytokine mRNA levels; these responses were accompanied by changes in NF-κB-associated proteins.

Macrophages serve as central sensors and orchestrators within the periodontal innate immune system, processing microbial cues and shaping the downstream cytokine microen-

vironment [10]. Upon encountering pathogen-associated molecular patterns (PAMPs) from *P. gingivalis*, macrophages polarize toward a pro-inflammatory phenotype, releasing various mediators and cytokines [7,10]. While these responses are initially defensive, their excessive and unresolved production drives maladaptive osteodestructive amplification loops within periodontal lesions [3,18]. In this study, pre-treatment with *P. kuromo* extract significantly suppressed NO production in *P. gingivalis*-stimulated RAW 264.7 macrophages. Extract-only treatment did not reduce RAW 264.7 cell viability at 15–60 μg/mL (Figure 2). However, viability was not assessed under the combined bacterial-stimulation and extract-treatment conditions; therefore, altered viability cannot be excluded as a contributor to the observed reductions in inflammatory markers.

NO, synthesized primarily via the iNOS pathway upon innate immune activation, acts as a double-edged sword in tissue pathology [4]. Under physiological homeostasis, basal NO contributes to localized antimicrobial defense; however, high-output, continuous generation by overactivated macrophages promotes oxidative stress, nitrosative cellular damage, and matrix metalloproteinase activation, thereby accelerating periodontal connective tissue degradation [4,11]. Consistent with the marked reduction in extracellular NO release observed in our Griess assays, Western blot analysis revealed that *P. kuromo* extract downregulated iNOS protein expression in a concentration-dependent manner (Figure 4). The reduction in nitrite accumulation was accompanied by lower iNOS protein expression. This association warrants further investigation in more physiologically relevant models.

Beyond transient gaseous mediators, the persistent upregulation of pro-inflammatory cytokines (notably TNF-α, IL-1β, and IL-6) is a hallmark of unresolved periodontitis [4,12]. From an osteoimmunology perspective, these cytokines link chronic tissue inflammation directly to alveolar bone loss. They not only amplify local leukocyte recruitment and vascular permeability but also upregulate receptor activator of NF-κB ligand (RANKL) while suppressing osteoprotegerin (OPG), thereby altering the RANKL/OPG ratio to promote pathological osteoclastogenesis and alveolar bone resorption [9]. In this study, *P. kuromo* extract markedly inhibited the mRNA expression of IL-1β, IL-6, and TNF-α under *P. gingivalis* stimulation (Figure 5). Whether these changes in cytokine mRNA levels translate into effects on periodontal tissue or bone resorption remains to be determined.

To examine whether NF-κB-associated protein changes were observed alongside the changes in inflammatory markers, we assessed selected proteins in this pathway [11]. In resting macrophages, the NF-κB p65/p50 heterodimer is retained in an inactive state in the cytoplasm by its inhibitory protein, IκBα. Pathogen-derived stimuli activate the upstream IKK complex, triggering phosphorylation of IKKα/β and IκBα, which targets IκBα for rapid ubiquitin–proteasome degradation and liberates NF-κB for nuclear entry [11,25]. At 24 h after exposure to the *P. gingivalis* preparation, the measured NF-κB-associated proteins and p65 distribution differed between stimulated and unstimulated cells. Extract treatment was associated with lower IKKα/β and IκBα phosphorylation, higher total IκBα levels, and reduced nuclear accumulation of p65 at this time point (Figure 6). These observations accompanied the lower inflammatory markers but do not establish a causal relationship. Because these proteins were assessed only at 24 h, the early kinetics of NF-κB signaling could not be determined.

As a crude extract, *P. kuromo* contains multiple constituents, as suggested by its HPLC profile (Figure 1). Marine macroalgae are known to contain compounds with potential immunomodulatory activity [19,26]. However, the chromatographic peaks detected in this study were not chemically identified, and the constituents responsible for the observed effects remain unknown. Although previous studies of marine algal compounds have proposed interactions with inflammatory signaling pathways [27,28], the present study did not assess direct binding to pattern-recognition receptors or IKK, nor did it determine whether

individual constituents act synergistically [29]. Moreover, because heat-treated whole *P. gingivalis* was used as the stimulus, these experiments cannot identify which bacterial components contributed to the observed response. Further chemical characterization and experiments with defined bacterial stimuli will be needed to investigate these possibilities.

Nevertheless, several limitations should be considered when interpreting these in vitro findings. First, although the RAW 264.7 macrophage cell line is widely used to study macrophage inflammatory responses, it does not capture the multicellular complexity of human periodontal tissue, including interactions among gingival fibroblasts, epithelial cells, periodontal ligament cells, and osteoblasts [10,30]. Studies using primary human periodontal cells would help evaluate the relevance of these findings in a more physiologically representative setting. Second, although we examined selected components of the NF-κB signaling pathway, other pathways, including mitogen-activated protein kinase (MAPK) cascades and NLRP3 inflammasome signaling, were not assessed and may contribute to the observed responses. Third, endotoxin activity was not measured in the *P. kuromo* extract or the heat-treated *P. gingivalis* preparation. Consequently, we cannot exclude endotoxin contamination of the extract or distinguish the contributions of bacterial cells and soluble components in the stimulus preparation. Cell viability was not assessed under the combined bacterial-stimulation and extract-treatment conditions; therefore, a contribution from altered cell viability to the reduced inflammatory markers cannot be excluded. Furthermore, the effects of the extract alone on nitrite accumulation, cytokine mRNA expression, and NF-κB-associated protein changes were not evaluated, and no positive anti-inflammatory reference treatment was included. These omissions preclude assessment of the extract's basal effects and direct comparison of its effects with those of an established agent. These limitations should be addressed in future studies.

5. Conclusions

In RAW 264.7 macrophages exposed to a heat-treated whole-bacterial preparation of *P. gingivalis*, *P. kuromo* extract reduced nitrite accumulation, iNOS protein expression, and the mRNA expression of IL-1β, IL-6, and TNF-α at the concentrations examined. Changes in IKKα/β and IκBα phosphorylation and the subcellular distribution of NF-κB p65 were also observed at 24 h, but these findings do not establish that the NF-κB-associated changes caused the reductions in inflammatory markers. Because cell viability was assessed with the extract alone, altered viability during combined exposure to the extract and bacterial preparation cannot be excluded as a contributor to the lower inflammatory markers. Whether these findings are relevant to periodontal disease should be evaluated in future studies using primary human cells and more physiologically relevant models. The present findings do not establish efficacy in periodontal tissue or therapeutic benefit.

Author Contributions: Conceptualization, H.-j.K.; methodology, M.-j.K. and H.-j.K.; investigation, M.-j.K. and T.Q.N.; data curation, M.-j.K. and H.-j.K.; writing—original draft preparation, M.-j.K. and T.Q.N.; writing—review and editing, H.-j.K.; visualization, M.-j.K. and T.Q.N.; supervision, H.-j.K. All authors have read and agreed to the published version of the manuscript.

Funding: This research received no external funding.

Institutional Review Board Statement: Not applicable.

Informed Consent Statement: Not applicable.

Data Availability Statement: The original contributions presented in the study are included in the article; further inquiries can be directed to the corresponding authors.

Acknowledgments: This work was supported by Wonkwang University in 2024.

Conflicts of Interest: The authors declare no conflicts of interest.

References

1. Kinane, D.F.; Stathopoulou, P.G.; Papapanou, P.N. Periodontitis. *Nat. Rev. Dis. Primers* **2017**, *3*, 17038.
2. Hajishengallis, G.; Lamont, R.J. Beyond the red complex and into more complexity: The polymicrobial synergy and dysbiosis (PSD) model of periodontal disease etiology. *Mol. Oral Microbiol.* **2012**, *27*, 409–419. [CrossRef]
3. Meyle, J.; Chapple, I.L. Molecular pathogenesis of periodontitis. *Periodontol. 2000* **2015**, *69*, 7–17. [CrossRef]
4. Pan, W.; Wang, Q.; Chen, Q. The cytokine network involved in the host response of periodontitis. *Int. J. Oral Sci.* **2019**, *11*, 30. [CrossRef]
5. Van Dyke, T.E. The resolution of inflammation in periodontitis. *Front. Immunol.* **2020**, *11*, 540192.
6. Serhan, C.N.; Levy, B.D. Resolvins in inflammation: Emergence of the pro-resolving superfamily of mediators. *J. Clin. Investig.* **2018**, *128*, 2657–2669. [CrossRef]
7. Hajishengallis, G. Periodontitis: From microbial immune evasion to systemic inflammation. *Nat. Rev. Immunol.* **2015**, *15*, 30–44. [CrossRef]
8. Tsukasaki, M.; Takayanagi, H. Osteoimmunology: Evolving concepts in bone-immune interactions. *Nat. Rev. Immunol.* **2019**, *19*, 626–642. [CrossRef]
9. Crotti, T.N.; Dharmapatni, A.A.; Alias, E.; Haynes, D.R. The role of receptor activator of nuclear factor-κB ligand (RANKL) and osteoprotegerin (OPG) in periodontal disease. *Periodontol. 2000* **2015**, *68*, 366–382.
10. Zhou, L.N.; Bi, C.S.; Gao, L.N.; An, Y.; Chen, F.; Cui, J.X. Macrophage polarization in periodontitis: Request for M1/M2 balance. *Front. Immunol.* **2019**, *10*, 1824.
11. Yu, T.; Ye, J.; Wang, R.; Wu, B.; Benjamin, S.; Sun, J. NF-κB signaling axis in periodontitis: From pathogenesis to therapeutic targets. *Int. Immunopharmacol.* **2023**, *118*, 110034.
12. Marchesan, J.; Girnary, M.S.; Jing, L.; Miao, M.Z.; Zhang, S.; Sun, L.; Offenbacher, S. An overview of gene expression in periodontitis: NLRP3 inflammasome activation. *J. Periodontol.* **2020**, *91*, 100–111.
13. Bartold, P.M.; Van Dyke, T.E. Host modulation therapy for periodontitis. *Periodontol. 2000* **2020**, *84*, 12–19.
14. Preshaw, P.M. Host modulation therapy with anti-inflammatory agents in periodontitis. *Periodontol. 2000* **2018**, *76*, 131–149. [CrossRef]
15. Chapple, I.L.; Mealey, B.L.; Van Dyke, T.E. Adjunctive therapies in the treatment of periodontitis: A critical review. *J. Clin. Periodontol.* **2022**, *49*, 124–142.
16. Sulijaya, B.; Takahashi, N.; Yamazaki, K. Host modulation therapy as a complement to mechanical debridement in periodontitis management. *J. Oral Biosci.* **2021**, *63*, 111–118.
17. Kirkwood, K.L.; Cirelli, J.A.; Rogers, J.E.; Giannobile, W.V. Novel host-modulating therapies for periodontitis. *Periodontol. 2000* **2007**, *43*, 238–253.
18. Garlet, G.P. Destructive and protective roles of cytokines in periodontitis: A re-appraisal from host defense and tissue destruction viewpoints. *J. Dent. Res.* **2010**, *89*, 1349–1363. [CrossRef]
19. Shannon, E.; Abu-Ghannam, N. Antibacterial and anti-inflammatory properties of marine macroalgae. *Mar. Drugs* **2019**, *17*, 356.
20. Choi, H.G.; Chun, J.; Choi, J.-Y.; Seol, H.-M.; Kim, E.G.; Kim, Y.; Lee, H.J.; Ahn, G.; Han, H.-S.; Shim, S.-Y. *Papenfussiella kuromo* Suppresses Lipopolysaccharide-Induced Inflammatory Mediator Release and Dextran Sulfate Sodium-Induced Colitis. *J. Nat. Polym.* **2026**, *31*, 114–120. [CrossRef]
21. Kang, O.-H.; Kim, S.-B.; Joung, D.-K.; Mun, S.-H.; Seo, Y.-S.; Kim, M.-R.; Shin, D.-W.; Choi, H.-G.; Kweon, K.-T.; Kwon, D.-Y. Anti-inflammatory effect of *Papenfussiella kuromo* in lipopolysaccharide or peptidoglycan-induced macrophage cells. *Afr. J. Pharm. Pharmacol.* **2012**, *6*, 2791–2797. [CrossRef]
22. Jia, L.; Han, N.; Du, J.; Guo, L.; Luo, Z.; Liu, Y. Pathogenesis of Important Virulence Factors of *Porphyromonas gingivalis* via Toll-Like Receptors. *Front. Cell. Infect. Microbiol.* **2019**, *9*, 262. [CrossRef]
23. Darveau, R.P.; Pham, T.-T.T.; Lemley, K.; Reife, R.A.; Bainbridge, B.W.; Coats, S.R.; Howald, W.N.; Way, S.S.; Hajjar, A.M. *Porphyromonas gingivalis* lipopolysaccharide contains multiple lipid A species that functionally interact with both Toll-like receptors 2 and 4. *Infect. Immun.* **2004**, *72*, 5041–5051. [CrossRef]
24. Kim, E.-N.; Nabende, W.Y.; Jeong, H.; Hahn, D.; Jeong, G.-S. The Marine-Derived Natural Product Epiloliolide Isolated from Sargassum horneri Regulates NLRP3 via PKA/CREB, Promoting Proliferation and Anti-Inflammatory Effects of Human Periodontal Ligament Cells. *Mar. Drugs* **2021**, *19*, 388. [CrossRef]
25. Liu, T.; Zhang, L.; Joo, D.; Sun, S.C. NF-κB signaling in inflammation. *Signal Transduct. Target. Ther.* **2017**, *2*, 17023. [CrossRef]
26. Shannon, E.; Conlon, M.; Hayes, M. Marine algae as an attractive source of functional ingredients for treatment of chronic inflammatory diseases. *Phytochem. Rev.* **2021**, *20*, 111–129.
27. Fitton, J.H.; Stringer, D.N.; Karpiniec, S.S. Therapies from fucoidan: New developments. *Mar. Drugs* **2015**, *13*, 6020–6046.
28. Besednova, N.N.; Andryukov, B.G.; Zaporozhets, T.S.; Kuznetsova, T.A.; Kryzhanovsky, S.P.; Ermakova, S.P.; Galkina, I.V.; Shchelkanov, M.Y. Molecular Targets of Brown Algae Phlorotannins for the Therapy of Inflammatory Processes of Various Origins. *Mar. Drugs* **2022**, *20*, 243. [CrossRef]

29. Caesar, L.K.; Cech, N.B. Synergy and antagonism in natural product extracts: When 1 + 1 does not equal 2. *Nat. Prod. Rep.* **2019**, *36*, 869–888. [CrossRef]
30. Bostanci, N.; Belibasakis, G.N. Delineating the inflammatory network of periodontal resident cells under bacterial challenges. *Front. Cell. Infect. Microbiol.* **2021**, *11*, 680214.

Disclaimer/Publisher's Note: The statements, opinions and data contained in all publications are solely those of the individual author(s) and contributor(s) and not of MDPI and/or the editor(s). MDPI and/or the editor(s) disclaim responsibility for any injury to people or property resulting from any ideas, methods, instructions or products referred to in the content.